



Contract № 3-2017 from 11th October 2017

LABORATORY TESTS OF GREENSTICK INCLINED WALL

Responsible administrant

Ph.D. Homitsky V.V.,

Ph.D. Meltsov G.I.

Kiev. 21th November 2018

Objective:

The research and analysis of hydromorphodynamic processes in the sea environment. The design of the enclosing structure is carried out in order to ensure its stability taking into account the existing hydrometeorological and hydrological conditions.

The tests were performed based on physical modeling of the dynamic factors taking into account new field data and choosing the optimal dimensions of the structural elements. The application field is maritime port and environmental construction.

1. The Experiment Automaton.

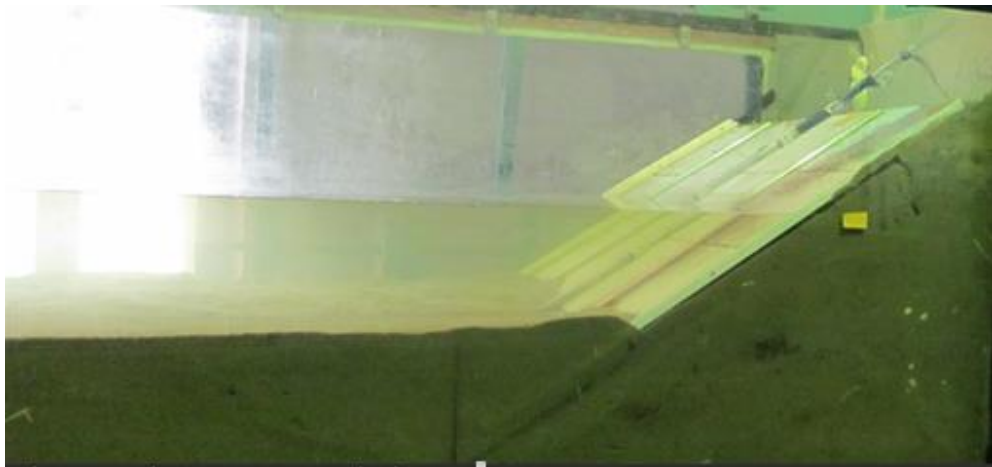


Figure 1. Greenstick wall model with pressure sensors

In the experiment were used measuring recording equipment, which allows to monitor continuously the wave flows that propagate in the wave channel and the operation of the wave generator. It also allows to change the operating mode of this

installation without shutting down. Along with the equipment that was created for the purpose of the registration of the wave pressure on the wall, also standard recording equipment was used. The use of these devices increased the reliability of this research work and helped to plan the experiment clearly.

The wave guide control system (Fig. 2.1), were used for the convenience of operation. The system is designed to control the wave generation in the research channel and provides the possibility of selecting and changing the main operating parameters: wave height; the oscillation period of the waveguide shield; the number of waves that have passed for a certain time; period of wave movement, as well as components that allow calculating of the propagation velocity and wave length.



a)



b)

Figure 2 System SRPX-1: a- external view without a computer, b-calibration of sensors; sensors placement on the model.

The SRPH-1 system (Fig. 2) was used for the registration and analysis of surface waves.

The system consists of surface wave sensors (DV) with connecting cables, an information conversion and transmission device (ISP), a communication line (LS), the personal computer information input/output device (PPW) combined with a power supply unit (PSU).

The system contains eight single surface sensors (DX). Double-threaded (M6) connection in DX design allows to use the sensors for recording waves both in deep water and in the coast zone.

DH installation in the coastal (near shore) zone is performed using special pins, which are screwed in and the handles (in duplicate). Verticality check of the DX installation is done by level "drop" built-in the handle.

The range of the recorded waves is ± 200 mm. The resolution is ± 1 mm.

The parameters of waves are transferred to a notebook personal computer. The surface waves data storage and display is done by the computer program "Volna M". The length of the connecting cables for the six wave sensors is 10 m, For the two DHs - 15 m. The length of the communication line between the SIP devices and the SIPM is 70 m. The length of the connecting cable between the PGPI and the personal computer PPVE is 0.4 m. PGPI and the personal computer PPVE are put in the separate box (construction) with dimensions not exceeding 80 x 140 x 200 mm with protection against dust and moisture of IP65 class. The power supply alternating current of 220 V /50 Hz from two 12 V batteries. The power consumption does not exceed 15 VA.

To record the wave height and length, were used capacitive sensors. This allows to obtain a rectilinear calibration characteristic within the range of produced waves (Fig. 2).

The sensors were placed at a distance of 1 m from each other.

The 4 pressure sensors were situated on the plastic panel of the Greenstick wall, and connected to the data collection and processing with the personal computer and the Oscill digital oscilloscope v.1.2.5 program, see Fig.3. Pressure sensors were fixed on a metal flat rod respectively fixed on the Greenstick wall panel, the lower sensor was located at the bottom level, each other with 10 cm interval up.

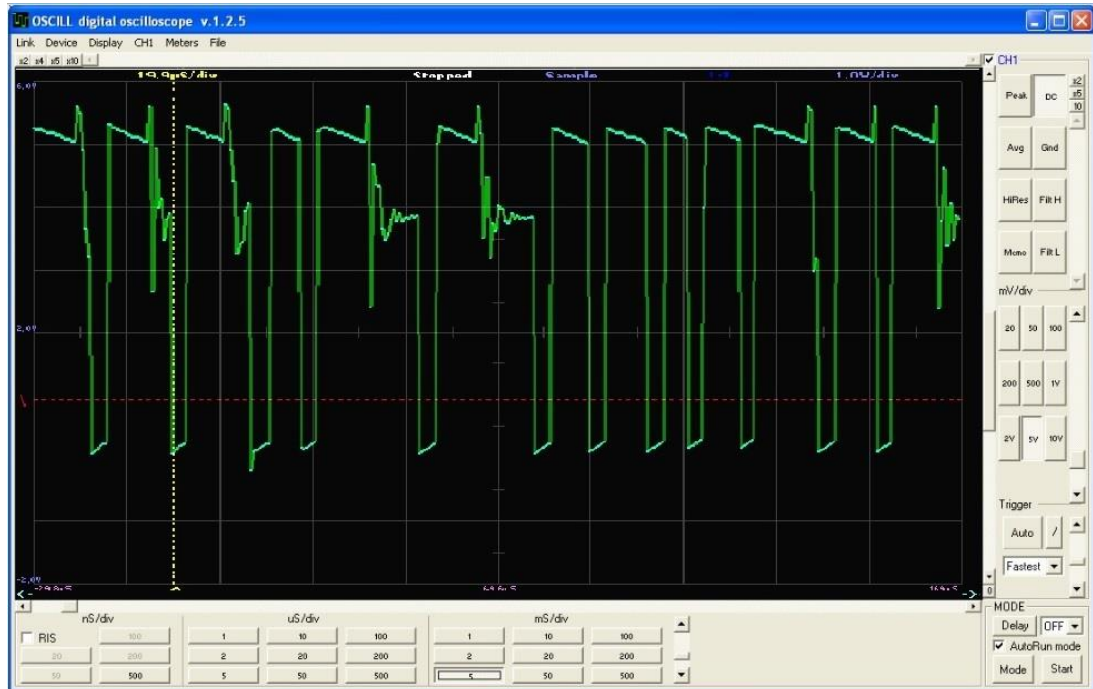


Figure 3. The Oscill digital oscilloscope program panel v.1.2.5

2. Methods of experimental studies.

Experimental studies on physical modeling were carried out in the wave tray of the Kiev Institute of Hydromechanics of National Academy of Science of Ukraine (Fig. 2). The length of the tray is 38 m, the width is 1 m, the depth is 0.7 m. The investigations were carried out under the conditions of monochromatic regular waves, which were destroyed when approaching the structure and on its contour.

3. Technique of conducting an experiment

1. Preparing the tray and equipment for the experiment.
2. Purchase of all necessary materials for building a model and conducting an experiment.
3. Configure and tune instruments and programs for measurement during the experiment.
4. Construction of the model.
5. Testing the model.
6. Experiment with different wave heights (you have a table that has wave heights) at a 30 degree incline.
7. Experiment with different wave height at 45 degrees incline.
8. Processing of experimental data.
9. Construction of graphs and tables.

The height of the waves produced by the wave-generator was controlled by changing the deviation angle of the shield plane from the vertical position. The frequency of the shield oscillations of the wave-generator (and, subsequently, the wavelength of the waves generated) were controlled by adjusting the resistance in the armature winding circuit.

A total of 22 experiments were conducted (see tables below).

Physical modeling, as a rule, is carried out on models, and is performed on a smaller scale. At the same time, it is important to evaluate the results obtained and the validity of their transfer to natural objects.

Unfortunately, existing methods of laboratory research are quite far from being complete, since in most cases it is impossible to provide similarity on models for all significant parameters. The published recommendations correspond to the current level of methodology development. In the future, with the accumulation of experimental data, numerical methods can be refined and supplemented.

It should be noted that the movement of sandy sediments (an average particle size of 0.1 ... 1 mm) is modeled approximately; therefore, in this case, natural data are valuable that can clarify the conditions of motion and sediment transport.

The wave mode is modeled in accordance with the Froude number, then the ratio between the wave parameters in full-scale conditions and on the model has the

form n_{B} , where n_{B} - vertical scale. The correlation of the wave periods on the model and in nature is $\sqrt{n_{\text{B}}}$.

The security of storms and levels is taken in accordance with existing regulatory documents.

The duration of the calculated storm is determined depending on the existing hydrometeorological situation in the area under study, the length of the period of operation of the artificial beach without repair replenishments and the existing along shore coastal sediment flow. The transverse horizontal scale of the underwater coastal slope (the scale of the beach width) is taken as distorted with respect to vertical scale $n_{\text{r}} = n_{\text{B}}^{1,35}$.

The scale of the model when studying the effect of transverse and longitudinal structures on the movement of sediments, the transformation of dumps (spilled in the surf zone), and also when studying the dynamics of coastal forms, the planned dimensions are commensurate with the width of the surf zone, are recommended to be corrected in the form

$$n_{\text{r}} = n_{\text{B}} = n_{\text{H}}^{1,35}.$$

It is recommended to set the transverse horizontal scale of subsurface structures, for example, breakwaters, or navigable canals over which the waves are transformed, adequate to wavelength scale.

The time scale for processing the model with n_{t} waves for the dynamics of the coastal zone, caused by the long-run sediment movement, is calculated according to the sediment balance equation by the dependence

$$n_{\text{t}} = \frac{n_{\text{H}} n_{\text{B}} n_{\text{r}}}{n_{\text{Q}}},$$

Moreover, the scale of the long-term sediment movement is determined by the ratio

$$n_{\text{Q}} = n_{\text{B}}^{2,3}.$$

When studying the processes of transverse deformation of the profile of the coastal slope under the influence of waves, it is assumed that $n_{\text{t}} = n_{\text{B}}$. The scale of the model's processing time by waves for processes in which transverse as well as long-range sediment transport are significant must be determined from the results of large-scale series, or field studies.

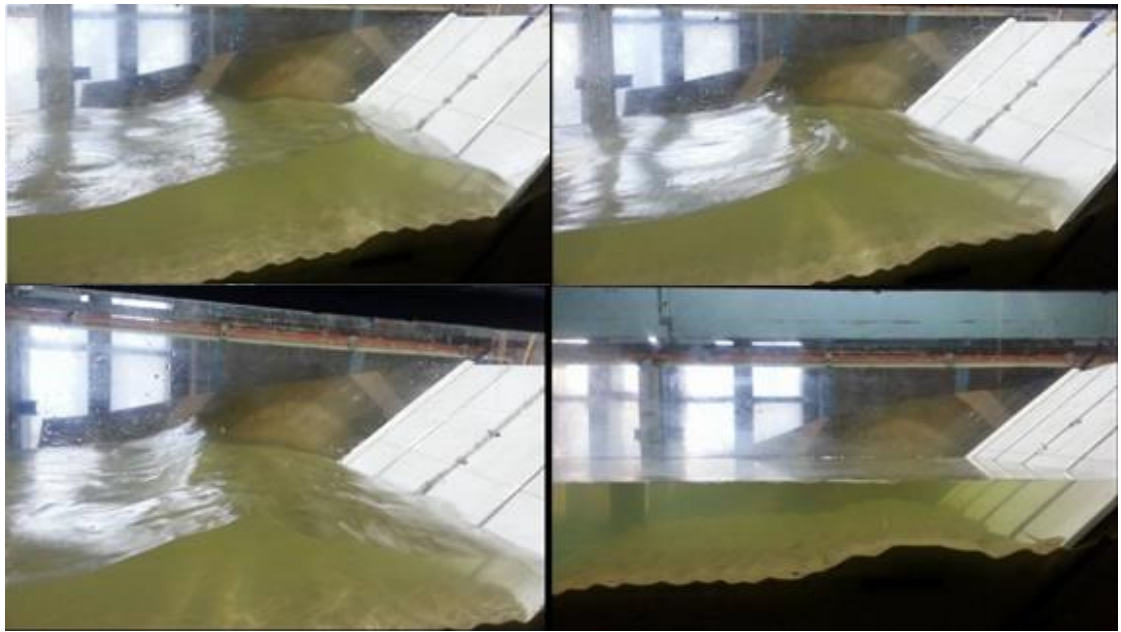
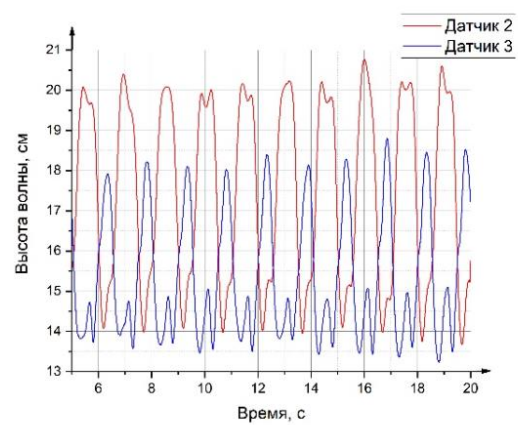
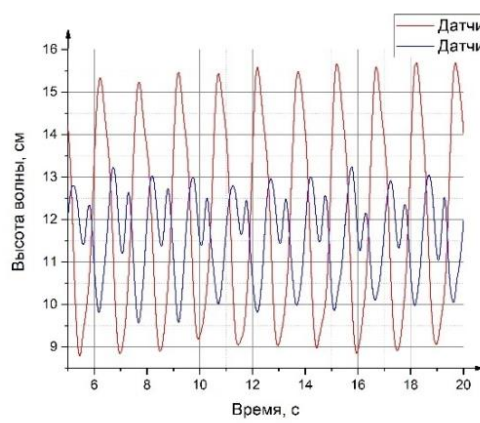
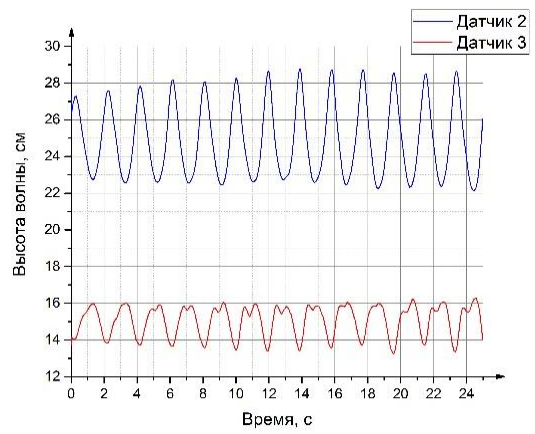
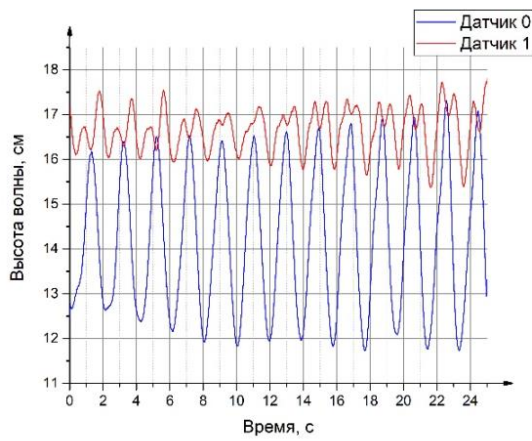
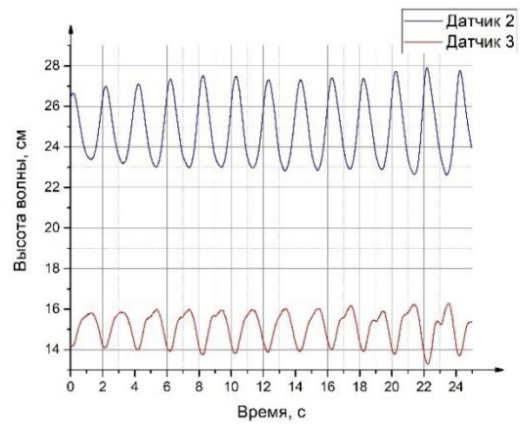
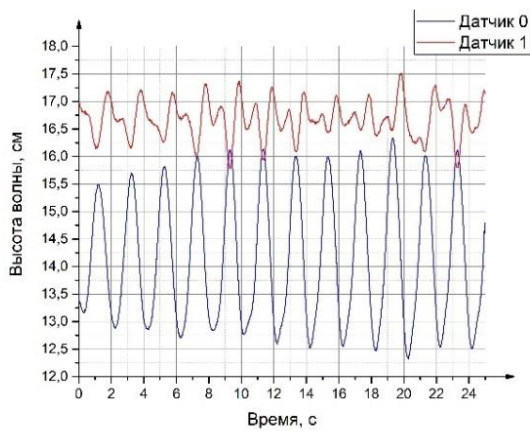
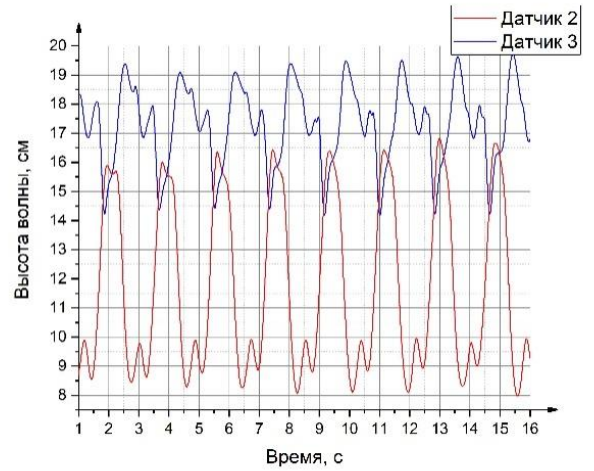
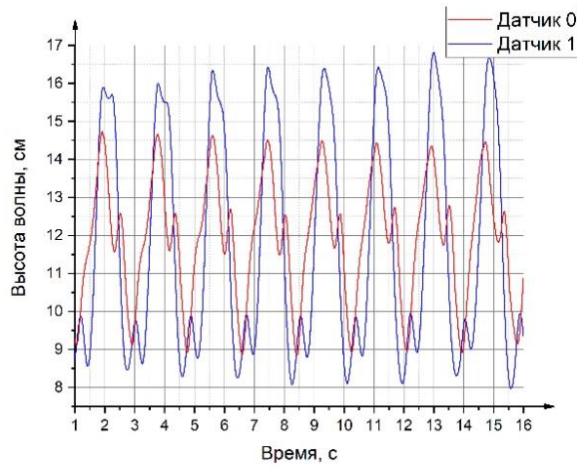


Figure 4. Swell/ripple formation on the bottom

4. Results of research

4.1 Waves parameters



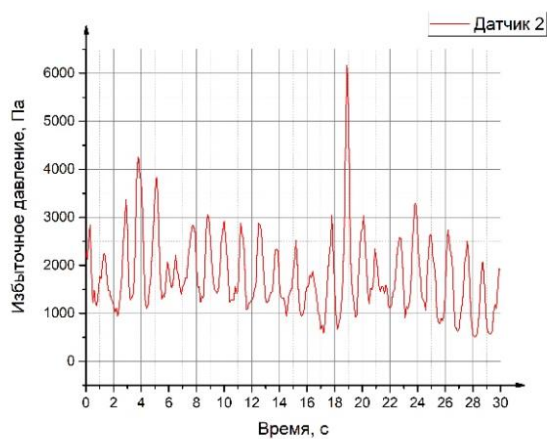
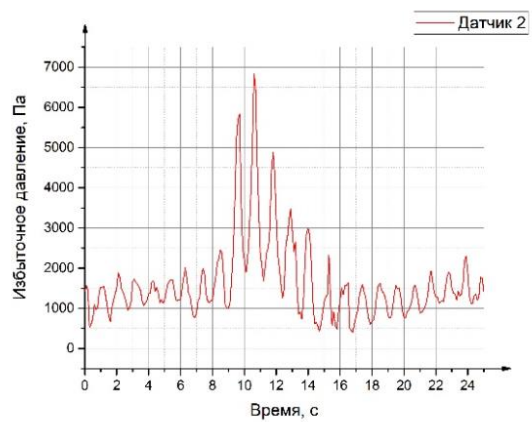
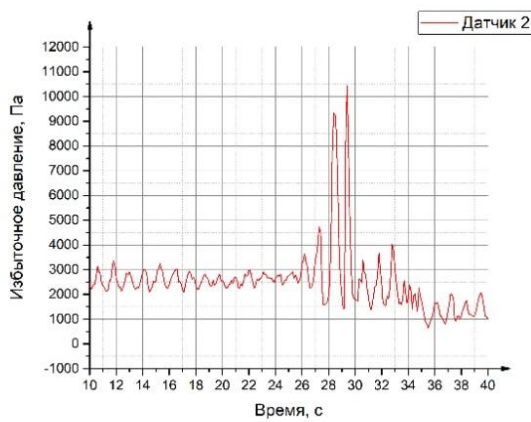
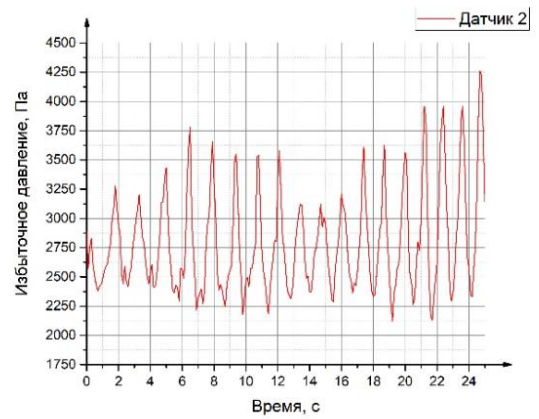
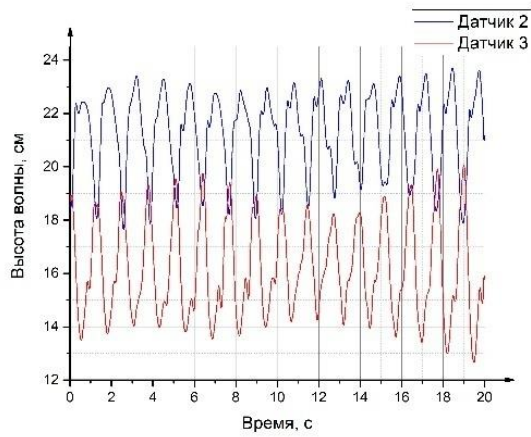


Experiment №	Gauge	Period, sec	Medium waves height, sm	min waves height, sm	max waves height, sm	Reflection rate	Waves height, m	Waves speed, m/sec
1	0	1,496	6,634	6,342	6,882	0,063	2,005 (2,626)	1,545 (2,024)
	1	1,099	3,237	2,836	3,528	0,156		
	2	1,499	6,358	6,072	6,866	0,123		
	3	1,498	4,896	4,351	5,588	0,143		
2	0	1,473	5,613	5,474	5,698	0,065	2,705 (4,259)	1,637 (2,578)
	1	1,831	8,206	7,544	8,633	0,101		
	2	1,378	5,21	4,742	5,577	0,136		
	3	1,039	4,779	4,624	4,996	0,085		
13_11_0 1	0	1,964	5,161	4,121	5,989	0,184	3,635 (6,014)	1,861 (3,063)
	1	1,615	1,941	0,383	3,065	0,737		
	2	1,963	5,614	3,643	7,332	0,395		
	3	0,73	0,819	0,274	1,699	0,846		
13_11_0 1	0	2,209	6,893	5,042	9,643	0,307	3,576 (7,611)	1,619 (3,446)
	1	1,81	4,151	2,829	5,45	0,185		
	2	2,209	9,832	9,249	10,389	0,118		
	3	1,25	3,799	2,592	5,012	0,685		
14_11_1	0	2,214	3,729	3,251	4,145	0,305	2,216 (8,346)	0,958 (3,608)
	1	2,375	6,308	5,79	7,071	0,185		
	2	2,412	8,377	7,849	9,122	0,136		
	3	1,863	4,315	3,917	4,585	0,224		
14_11_1 st	0	1,643	12,966	7,891	18,173	-	-	-
	1	1,216	7,326	2,75	13,758	-		
	2	1,656	13,304	5,215	22,158	-		
	3	0,939	8,153	2,159	21,178	-		
14_11_2	0	1,75	8,531	4,789	11,788	0,602	3,241 (5,13)	1,787 (2,829)
	1	1,686	7,412	4,582	14,818	0,569		
	2	1,877	10,255	8,794	12,955	0,122		
	3	1,491	6,57	3,501	14,296	0,724		

Experiment №	Gauge	Period, sec	Medium waves height, sm	min waves height, sm	max waves height, sm	Reflection rate	Waves height, m	Waves speed, m/sec
14_11_2_1	0	1,524	17,873	15,179	21,314	0,195	1,873 (3,538)	1,244 (2,349)
	1	1,544	20,726	19,38	22,519	0,123		
	2	1,488	15,053	11,483	17,513	0,282		
	3	1,423	14,948	11,058	18,272	0,323		
14_11_3	0	3,755	8,035	7,464	8,877	0,167	1,7 (17,761)	0,504 (5,264)
	1	2,993	5,406	4,663	6,004	0,186		
	2	2,168	3,036	1,774	4,051	0,51		
	3	3,575	7,702	7,078	8,326	0,236		
14_11_3st	0	3,189	8,485	1,904	11,186	-	-	-
	1	2,987	5,094	3,431	7,067	-		
	2	1,625	3,584	2,544	5,137	-		
	3	4,064	10,384	9,49	11,618	-		
14_11_3_01st	0	2,595	8,302	5,281	11,304	-	-	-
	1	2,542	1,177	4,916	9,312	-		
	2	1,907	5,438	3,655	8,033	-		
	3	3,352	8,487	5,448	10,531	-		
14_11_4	0	1,385	6,253	5,762	6,923	0,134	1,503 (3009)	1,082 (2,167)
	1	1,393	4,31	3,766	5,023	0,321		
	2	0,785	1,18	0,689	1,42	0,527		
	3	1,368	3,036	2,257	3,723	0,286		
14_11_4_01	0	1,317	5,744	4,832	6,424	0,205	2,285 (2,608)	1,767 (2,017)
	1	1,19	3,327	2,177	4,747	0,442		
	2	1,268	2,897	2,418	3,53	0,377		
	3	1,317	3,753	2,751	3,342	0,156		

Experiment №	Gauge	Period, sec	Medium waves height, sm	min waves height, sm	max waves height, sm	Reflection rate	Waves height, m	Waves speed, m/sec
14_11_5	0	0,676	3,513	2,306	4,387	0,515	0,331 (0,638)	0,517 (0,997)
	1	0,603	3,413	2,159	4,025	0,341		
	2	1,17	5,794	5,507	6,234	0,173		
	3	1,244	5,379	4,306	7,058	0,317		
14_11_6	0	1,304	4,88	4,342	5,302	0,14	2,197 (2,242)	1,833 (1,87)
	1	1,093	2,978	2,722	3,186	0,132		
	2	1,306	3,155	2,624	3,67	0,122		
	3	1,304	4,219	3,923	4,684	0,114		
14_11_6 otr	0	1,279	4,687	3,726	5,539	0,395	1,041 (2,545)	0,815 (1,992)
	1	0,751	2,263	1,358	2,816	0,448		
	2	1,275	4,977	4,586	5,635	0,245		
	3	1,271	5,612	5,275	6,03	0,174		
14_11_o tr_1	0	0,68	4,484	3,361	6,07	0,399	0,373 (0,658)	0,274 (1,013)
	1	0,619	4,506	3,058	6,57	0,404		
	2	1,227	7,248	5,787	9,839	0,211		
	3	1,237	7,705	5,106	10,756	0,438		
23_11_1	0	1,897	3,388	2,021	3,999	0,156	3,784 (5,949)	1,938 (3,046)
	1	1,107	1,189	0,335	1,757	0,744		
	2	2,008	4,653	3,739	5,386	0,176		
	3	1,402	1,75	0,135	3,069	0,915		
23_11_2	0	1,836	4,574	2,365	5,651	0,21	3,705 (5,517)	1,97 (2,934)
	1	1,064	1,273	0,239	2,538	0,833		
	2	1,925	6,019	5,063	6,456	0,171		
	3	1,73	2,418	1,659	2,843	0,909		

4.2 Pressures dependence on wave parameters



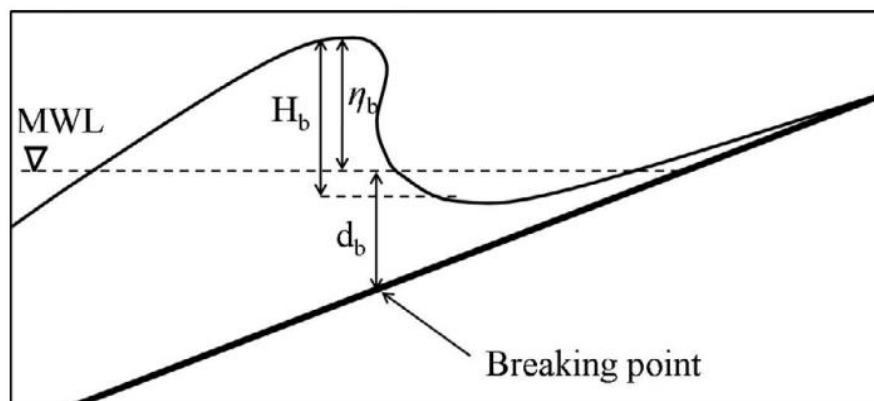
4. Computational model of wave pressure on inclined wall []

4.1.1 Wave breaking

Wave breaking is generally caused by several mechanisms, but in the terms of dike breaching, the most important are related to the influence of shallow water. In the frames of this work, the wave breaking due to wind action or wave-wave interaction is neglected. In principle, the wave breaks, when the orbital velocity at the surface (u_{ob}) is larger than the wave celerity (c), the wave reaches its terminal steepness and the angle of the wave peak is smaller than 120° .



(a) Wall model in the wave flume



(b) Wave breaking on a slope - principle sketch Figure 6 Breaking wave on a dike slope

In Fig. 6a the picture of wave breaking in a wave flume is given, while Fig. 6b shows schematically the geometry of a breaking wave. The type of the wave breaking is estimated using the surf similarity parameter (e.g. Battjes, 1974):

$$\xi = \frac{\tan \alpha}{\sqrt{\frac{H}{L_0}}} \quad \text{with} \quad L_0 = \frac{gT^2}{2\pi} \quad (1)$$

where:

- ξ - surf similarity parameter [-]
- α - outer wall slope [deg]
- H - wave height at the wall toe [m]
- L_0 - deep water wave length [m]
- T - wave period [s]

Three forms of wave breaking can be distinguished (i) surging breaker, (ii) plunging breaker and (iii) spilling breaker (Table 1)

Dike slope 1:n	Plunging breaker	Collapsing breaker	Surging breaker
1:6	$\xi < 2.1$	$2.1 < \xi < 2.8$	$\xi > 2.8$
1:4	$\xi < 2.4$	$2.4 < \xi < 3.1$	$\xi > 3.1$
1:3	$\xi < 2.6$	$2.6 < \xi < 3.3$	$\xi > 3.3$
mean	$\xi < 2.3$	$2.3 < \xi < 3.0$	$\xi > 3.0$

Table 1. Classification of breaking types on sea dikes (Schüttrumpf, 2001)

In terms of dike breaching, a plunging breaker represents the most crucial type of the wave breaking. The wave energy is dissipated over a short distance and within

a short time, which results in relatively small surfaces exposed for a very short period of time (0.01 to 0.1 s) to very high impact pressures (up to 150 kPa). This impact load does not act continuously, but intermittently in time intervals of at least one wave period (usually longer with predominant impact on the water layer that results from the wave up and down rush process of the preceding wave). Therefore, the actual loading time (0.1 to 0.01 s) is small in comparison with the time period between the loads (5-12s). The wave breaking process is subject to strong variations due to the influence of the entrained air, so the parameters describing this process have to be described stochastically.

4.2 Location of the impact on the dike slope.

The location of the impact on the dike slope can be calculated using the following formula proposed by Schüttrumpf and Oumeraci (2005):

$$\frac{Z_{impact}}{H} = h_{MWL} - 0.8 + 0.6 \cdot \tanh(\xi - 2.1) \quad (2)$$

where impact Z is defined as in Fig. 7

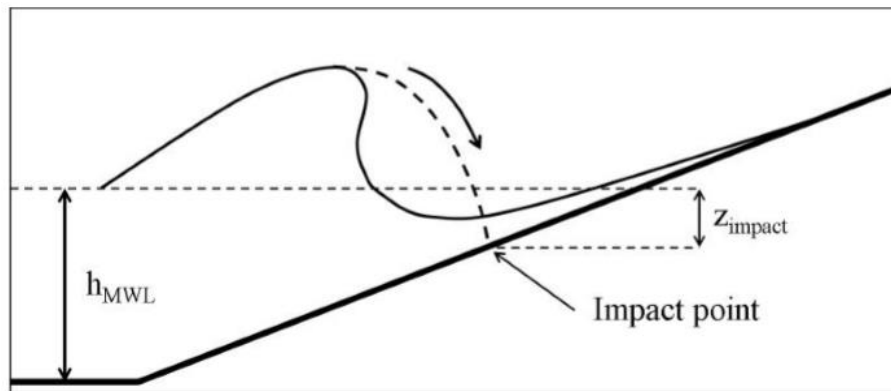


Figure 7 Location of the impact on a slope - principle sketch

This empirical formula is associated with a satisfying degree of uncertainty (20% = σ') and can be applied for both regular waves and irregular waves.

4.3 Impact pressures

The impact pressures on the slope are subject to very large spatial and temporal variations which make the impact load a highly stochastic process. Even in a regular wave train the impact pressures significantly differ for every single wave. Due to the complex characteristics of this problem, research was performed mostly experimentally, in the area of medium- and large scale models (TAW, 1990). Since the maximum impact pressure is a stochastic variable, the maximum impact pressure has to be defined more specifically. To indicate the maximum pressure that is not exceeded in i % of the cases, the notation $p_{max,i}$ is used. In practice p_{max99i} is considered as the highest measured maximum impact pressure.

For the implementation in the preliminary model the modified approach proposed by Führböter and Sparboom (1988) is selected:

$$p_{max,i} = const_i \cdot \rho_w \cdot g \cdot H \cdot \tan \alpha \quad (3)$$

with:

g - acceleration due to gravity [$\frac{m^2}{s^2}$]

ρ_w - density of the water [$\frac{kg}{m^3}$]

$const_i$ - coefficient depending on the characteristic maximum value considered [-]

- $const_{50} = 12$

- $const_{90} = 16$

- $const_{99} = 20$

- $const_{99,9} = 30$

The decrease of the impact pressure on a flatter dike slope is the result of the damping effect of the water layer resulting from the run-down of the preceding wave. The thickness of this back-rush water layer increases with flatter slope so that the maximum pressures decreases proportionally. Another effect of the dike slope angle

is the number of breaking waves generating an impact pressure. For steeper slopes and the same incident waves the surf-similarity parameter ξ is smaller, and another breaking regime may occur with less breaking waves per unit of time. This was reported by Bölke and Relotius (1974) and Führböter et al (1976), who presented time series of impact pressures based on simultaneous measurements during a storm surge in 1973. The conclusion states that the number of waves generating impact pressures is much lower for a slope 1:6 than for a slope 1:4. The influence of the wave steepness on the maximum impact pressure is however not taken into account. This serious drawback can be eliminated using instead of the constant value κ_i in Eq. (3) an empirical function k_i that depends on the wave steepness (Zhong, 1985):

$$P_{max,i} = \kappa_i \cdot \rho_w \cdot g \cdot H \cdot \tan\alpha \quad (4)$$

with:

$$\kappa_{50} = -289 \cdot \frac{H}{g \cdot T^2} + 11.2 \quad (5)$$

and:

$$k_{90} = 1.33 \cdot k_{50}$$

$$k_{99} = 1.67 \cdot k_{50}$$

$$k_{99,9} = 2.5 \cdot k_{50}$$

In Fig. 8 the comparison of measured results with Eq. (4) together with Eq. (5) is shown.

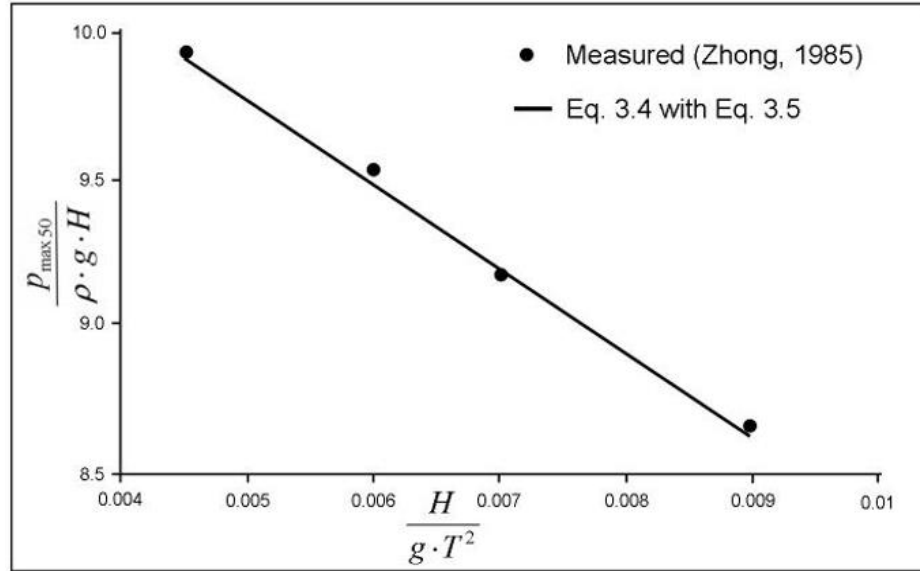


Figure 8 Dependency of the impact pressure on the wave steepness

4.4 Distribution of the impact pressures on the wall slope

For the preliminary model the following formula for the impact pressure on a point with given coordinates x_i and z_i is used (after Stive, 1983) :

$$P_i = \left[-\frac{2.75}{H^2} \cdot ((z_i - z_{impact})^2 + (x_i - x_{impact})^2) + 1 \right] \cdot P_{max} \quad (6)$$

with:

- x_i and z_i - coordinates of the i -th point
- x_{impact} and z_{impact} - coordinates of the impact point calculated as:
 - $z_{impact} = MWL - Z_{impact}$
 - $x_{impact} = z_{impact} \cdot \tan \alpha$

Eq. (6) gives a negative impact pressure for the distance d_i between the i -th point and the point of impact larger than the maximal distance d_{max} (Fig. 9):

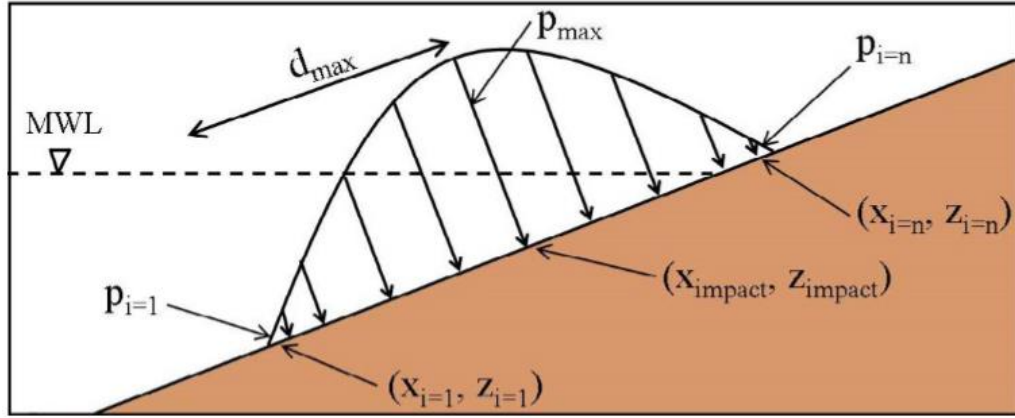


Figure 9 Impact pressure distribution on the wall slope

To avoid this problem, the limits are introduced (Fig. 9)

$$d_i = d_i \quad \text{for} \quad |d_i| < d_{max}$$

$$d_i = 0 \quad \text{for} \quad |d_i| > d_{max}$$

with max d calculated as:

$$d_{max} = \frac{H}{\sqrt{2.75}} \quad (8)$$

Eqs. (6)-(8) were derived based on the results of large-scale tests reported by Stive (1983). It is however strongly simplified and gives a deterministically described distribution of the pressures.

4.5 Incidence angle of plunging wave impact The angle of incidence of the breaking wave plunging on the dike slope (Fig. 10) is calculated using the approach proposed by Führböter (1966). This theoretical formula gives the angle impact α as a function of the seaward slope angle α and reads:

$$\alpha_{impact} = atan\left(\frac{1 + \cot\alpha \cdot f(\alpha)}{\cot\alpha - f(\alpha)}\right) \quad (9)$$

with:

$$f(\alpha) = \frac{\sqrt{1 + 2\cot^2 \alpha} - 1}{\cot \alpha} \quad (10)$$

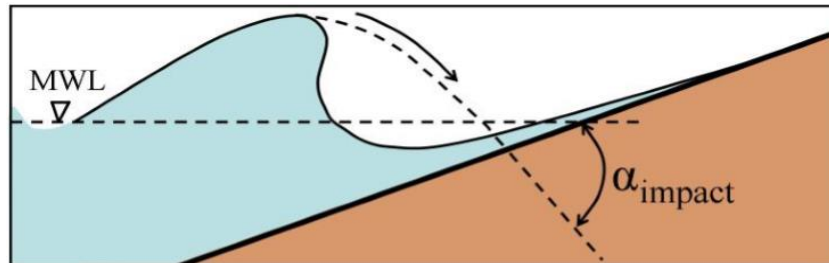


Figure 10 Incidence angle of plunging wave impact (after Führböter, 1966)

Conclusions

In the experiments with the physical model, the Greenstick inclined wall was considered. It is used in marine port and environmental construction in shallow waters. This design for certain conditions is more optimal and cost-effective. The stability of the structure is not analyzed for the effect of ice loads.

Results of experiments demonstrated, that measured waves pressure good enough correspond to pressures calculated with traditional analytical methods.

Incline of Greenstick wall provides considerable decline of:

- wave pressure on the wall;
- bottom score in front of the wall.

Minimisation of waves pressure and score is proportional to the angle of incline of Greenstick wall.

Experiments demonstrated, that Greenstick wall due to sheeted and tilted surface may be used in port and environment construction for: embankments, dams, levees, dikes, sea walls, e.t.c. and is more reliable and cost-effective as traditional soil surfaces, and reinforced by concrete, asphalt concrete, and other mattresses, purred polyurethane, e.t.c.

For ice zones, additional tests of Grenstick wall must be provided for prove of resistibility of structure to ice loads.

References

- WEST, D.; MELTSOV, G. Mooring device and articulated structures. GB Patent. Grenstick, 2013, 144pp.
<http://patentscope.wipo.int/search/en/detail.jsf?docId=WO2013150276&recNum=6&maxRec=&office=&prevFilter=&sortOption=Pub+Date+Desc&queryString=&tab=PCT+Biblio>
- Sea Dike Breaching Initiated by Breaking Wave Impact Preliminary computational model
- BATTJES, J.A. (1974): Computation of set-up, longshore currents, run-up and overtopping due to wind-generated waves, Ph.D. Thesis, Delft University of Technology, Civil Engineering Department, Delft, The Netherlands, 244 pp
- SCHÜTTRUMPF, H.; OUMERACI, H. (2005): Layer thicknesses and velocities of wave overtopping flow at seadikes. Coastal Engineering vol. 52(no. 6): pp. 473-495
- BOELKE, S., RELOTIUS P.C.(1974): Über die wellenerzeugten Druckschlagbelastungen von Seedeichen im Böschungsbereich zwischen 1:4 und 1:6. Mitteilungen Leichtweiß-Institut für Wasserbau der Technischen Universität Braunschweig Heft 42: pp. 358-388.
- FÜHRBÖTER, A.; DETTE, H.-H.; GRÜNE, J. (1976): Response of seadykes due to wave impacts, Proceedings 15th International Conference Coastal Engineering (ICCE), Honolulu, Hawaii, pp. 2604-2622
- ZHONG, H., (1985): Theoretische und experimentelle Untersuchungen ober den Druckschlag bei Wellenangriff auf einen 1:4 geneigten Seedeich. Mitteilungen des Leichtweiß- Institut für Wasserbau, Techn. Univ. Braunschweig, pp.401-453
- STIVE, R.J.H. (1983): Internal note, Delft Hydraulics (quoted by TAW, 1990)
- FÜHRBÖTER, A. (1966): Der Druckschlag durch Brecher auf Deichböschungen, Mitteilungen des Franzius-Instituts für Grund- und Wasserbau der Technischen Universität Hannover, Heft 31